Computational Study of CO_2 Reduction by Amines†

Barry K. Carpenter‡

Department of Chemistry and Chemical Biology, Baker Laboratory, Cornell University, Ithaca, New York 14853-1301

Received: September 14, 2006; In Final Form: October 8, 2006

Calculations at the MP2/aug-cc-pVDZ//MPWB1K/aug-cc-pVDZ level are reported for the reduction of CO_2 by amines—primarily triethylamine. A polarizable continuum model is used to represent acetonitrile solvent for the reaction. Starting from a photochemically generated radical ion pair state, the mechanism of reduction is deduced to be one in which the $CO_2^{\bullet -}$ begins to use one of its oxygens to abstract a hydrogen from an α carbon of the amine radical cation. During this event, and before the transition state for H transfer is reached, the system encounters a surface crossing, which provides pathways for unproductive back electron transfer and for productive reduction, with the latter involving attachment of the hydrogen to the *carbon* of CO_2. The result of the reduction is a closed-shell iminium formate ion pair, which completes the reaction by proton transfer between the ions, to give an eneamine and formic acid. On the basis of the calculations, approaches for improving the efficiency of the reduction and increasing the wavelength of the light used to drive the reaction are discussed. One of these modifications involves the use of a bicyclic amine as reductant.

Introduction

Despite political skepticism from certain quarters, the objective evidence in support of a deleterious effect of anthropogenic CO_2 on the climate of this planet is overwhelming.[1] Consequently, the search is now on for ways to slow the increase in atmospheric CO_2 concentration. Those efforts include attempts to replace the combustion of fossil fuels as sources of energy,[2] as well as investigations into removal some of the excess CO_2 already in the atmosphere.[3] The photochemical reduction of CO_2 could potentially make a contribution to both of these approaches, because the reduction products could be compounds whose combustion would provide energy while being overall neutral in their effect on the CO_2 burden.[4] If the photochemistry could be conducted with sunlight, one would in principle have a means for converting solar energy into a transportable fuel, although a host of issues would obviously need to be addressed to make such a scheme economically viable.

Among those issues is the fact that the only economically sensible reductant for the CO_2 is water. Nevertheless, other reductants, such as amines, can be considered, provided they can be regenerated in schemes that ultimately involve the oxidation of water. A principal goal in the present computational study was to elucidate issues in amine/CO_2 redox chemistry that could help in the design of reaction chains linking the reduction of CO_2 and the oxidation of water. Toward that end, much of the computational effort centered on triethylamine, which is known to be capable of photochemically reducing CO_2,[5−10] with a view to determining how the reaction works, and hence what might be done to make it work better. However, some of the more complex and computationally demanding details were studied with the smaller model of methylamine as the reducing agent.

The photochemical reduction of carbon dioxide has been studied quite extensively in heterogeneous[11−13] and homogeneous systems, and for the latter with organic[14] as well as transition-metal based[5,10] photocatalysts. Despite this history, the details of the reduction steps have received little theoretical attention. This paper seeks to rectify that situation, at least partially, by focusing on the reduction of CO_2 in polar solvents, with amines as the sacrificial reductants. The analysis begins with the charge-transfer state in which the photocatalyst has effected the net transfer of an electron from the amine to the CO_2. The conclusions are therefore obviously of no relevance to CO_2 reduction schemes that follow different mechanisms.

Computational Methods

The search for a computational model that would provide a reasonable compromise between accuracy and tractability was undertaken by comparison of several candidates on the prototype reaction between methylamine and CO_2. With the available hardware, the largest basis set that would be feasible for the full calculations on triethylamine + CO_2 was judged to be aug-cc-pVDZ,[15] and so that basis set was used in the prototype calculations. The electronic-structure models considered for evaluation were the common hybrid DFT method B3LYP,[16] the MPWB1K density functional from Truhlar's group,[17] and second-order Møller−Plesset theory (MP2).[18] Initially, these were compared for thermochemical accuracy against CBS-APNO,[19] using the computed reaction enthalpies of various gas-phase hydrogen-transfer reactions from the methyl group of CH_3NH_2 to CO_2.

Unscaled harmonic vibration frequencies were used in the enthalpy calculations for the B3LYP, MPWB1K, and MP2 models, because the study of Scott and Radom has shown that the best scale factors for vibrational contributions to enthalpy are very near unity with the B3LYP and MP2 models.[20] It was assumed that the same would be true for the MPWB1K density functional. The results are shown in Table 1. The rms deviations between the results for each of the three test models and those

† Part of the special issue "James A. Miller Festschrift".

‡ E-mail: bkc1@cornell.edu. Present address: School of Chemistry, Cardiff University, Main Building, Park Place, Cardiff CF10 3AT, Wales, U.K.

10.1021/jp0660076 CCC: $37.00
Published on Web 12/07/2006

TABLE 1: Calculated Reaction Enthalpies (kcal/mol) at 298 K for Various Gas-Phase Hydrogen Transfers from Methylamine to CO_2[a]

reaction products	CBS-APNO	B3LYP	MPWB1K	MP2
$HCO_2^- + H_2C{=}NH_2^+$	167.0	162.7	166.1	167.7
$HCO_2^{\bullet} + H_2C^{\bullet}{-}NH_2$	105.7	93.0	99.7	108.4
trans-$HOCO + H_2C^{\bullet}{-}NH_2$	90.8	83.6	86.8	94.3
$HCO_2H + HC{-}NH_2$ ($^1A'$)	66.4	62.2	64.1	70.1

[a] The B3LYP, MPWB1K, and MP2 calculations all used the aug-cc-pVDZ basis set.

for CBS-APNO were found to be 7.9, 3.8, and 2.9 kcal/mol for B3LYP, MPWB1K, and MP2, respectively.

It is perhaps worth noting in passing that the calculations revealed the possibly surprising conclusion that, in the gas phase, the least endothermic hydrogen transfer from the methyl group of methylamine to CO_2 involves exchange of two hydrogens rather than one, affording formic acid and singlet aminomethylene. The least endothermic transfer of a single hydrogen was the one yielding *trans*-HOCO and $H_2N{-}CH_2^{\bullet}$. The overall greater favorability of the double hydrogen transfer can be attributed to two components: the C−H bond dissociation enthalpies (BDEs) of methylamine and the H-atom affinities of CO_2. For methylamine, CBS-APNO gave a first C−H BDE of 93.3 kcal/mol and a second of 73.7 kcal/mol. This order stands in striking contrast to the corresponding values for methane, which has experimental first and second BDEs of 105.0 and 110.4 kcal/mol, respectively.[21] The very low C−H BDE of $H_2N{-}CH_2^{\bullet}$ can be attributed to the now well-recognized[22] stabilizing interaction of the nitrogen lone pair in the singlet carbene product from H-atom loss. For CO_2, CBS-APNO afforded first and second H-atom affinities of 2.5 and 98.1 kcal/mol, respectively. It is the fact that the second H-atom affinity of CO_2 exceeds the second C−H BDE of methylamine that leads to the double hydrogen transfer being favored.

The next step in the assessment of computational models was to evaluate their performance with dielectric-continuum corrections for solvent effects. The polarizable continuum (PCM)[23] model, utilizing a united-atom foundation for definition of the cavity was employed. To this was added an explicit sphere around the migrating hydrogen in each of the H-transfer reactions. Composite electronic-structure models, such as CBS-APNO, cannot currently incorporate solvent corrections. Consequently, a CCSD calculation, which is the highest-level correlated method for which PCM corrections are readily available, was used as one reference against which lower-level models could be judged. A second reference was provided by an MP2 calculation with the larger aug-cc-pVTZ basis set. Again, the methylamine−CO_2 reaction was used in the assessment, but this time only the hydride transfer was studied because, in the polar media of principal interest for the present study, it turned out to be the least endothermic reaction of the four listed in Table 1. Because the geometry optimizations and frequency calculations were considerably slower when the solvent corrections were included, only the two DFT models were used in those steps. Single-point MP2 or CCSD calculations were then carried out on the DFT stationary points. Finally, because barrier heights as well as overall reaction thermochemistry would be of importance in the full study, the activation enthalpy for the hydride transfer was used as the assessment metric. The built-in Gaussian 03 representations of the solvents dichlorethane, dichloromethane, ethanol, methanol, acetonitrile, nitromethane, and dimethyl sulfoxide were investigated. The results are summarized in Figures 1 and 2.

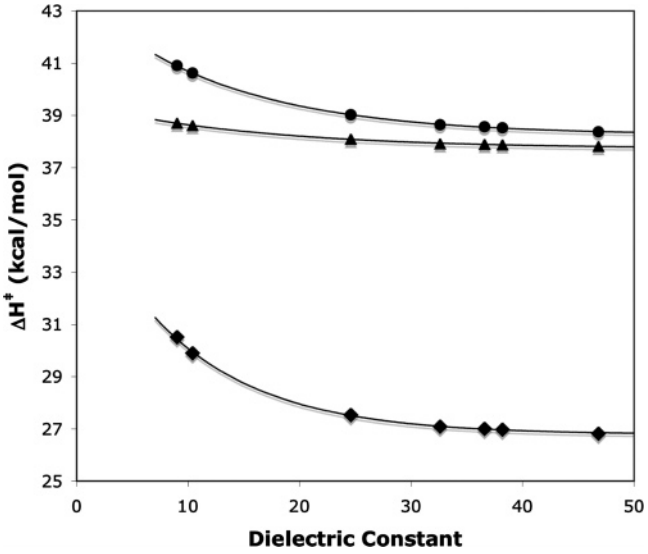

Figure 1. Calculated activation enthalpies for the hydride-transfer reaction $H_2N{-}CH_3 + CO_2 \rightarrow H_2N^+{=}CH_2 + HCO_2^-$ in solvents of different polarity, using the PCM model. Geometry optimizations and vibrational frequency calculations were carried out at the B3LYP/aug-cc-pVDZ level, including the solvent corrections. Key: ◆, B3LYP/aug-cc-pVDZ; ▲, CCSD/aug-cc-pVDZ; ●, MP2/aug-cc-pVTZ. The curves are designed to help visualization of the graph but have no theoretical significance.

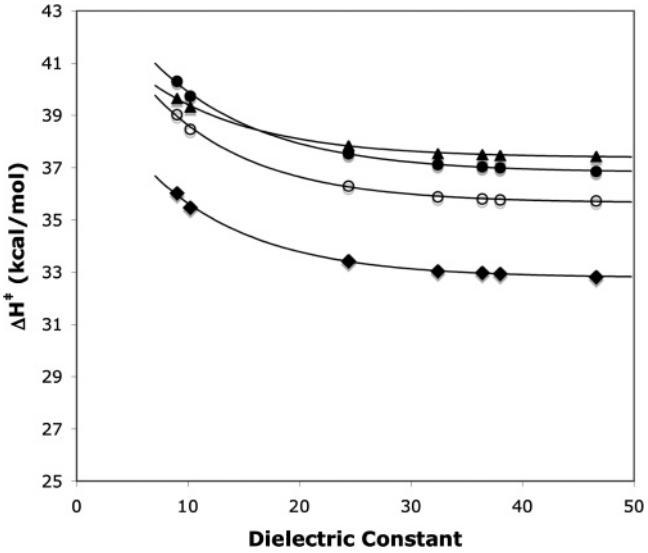

Figure 2. Calculated activation enthalpies for the hydride-transfer reaction $H_2N{-}CH_3 + CO_2 \rightarrow H_2N^+{=}CH_2 + HCO_2^-$ in solvents of different polarity, using the PCM model. Geometry optimizations and vibrational frequency calculations were carried out at the MPWB1K/aug-cc-pVDZ level, including the solvent corrections. Key: ◆, MPWB1K/aug-cc-pVDZ; ○, MP2/aug-cc-pVDZ; ▲, CCSD/aug-cc-pVDZ; ●, MP2/aug-cc-pVTZ. The curves are designed to help visualization of the graph but have no theoretical significance.

As the graphs in Figures 1 and 2 reveal, the DFT models were found to underestimate the activation enthalpies significantly with respect to those computed with the CCSD and MP2 methods. The problem was particularly severe for B3LYP, which gave barrier heights roughly 10 kcal/mol lower than those from the reference calculations. Together, the results from the gas-phase enthalpy calculations and the solution-phase activation-barrier calculations suggested that the best compromise among the methods selected for study was MP2/aug-cc-pVDZ//MPWB1K/aug-cc-pVDZ. The results in Figure 2 indicate that barriers computed with this model might be systematically

underestimated by about 2 kcal/mol with respect to those from the higher level methods.

In the calculations on triethylamine + CO_2, the PCM model for acetonitrile was used, and all geometry optimizations and vibrational frequency calculations were carried out with the solvent correction. All calculations used the Gaussian 03 suite of programs.[24]

Results and Discussion

Elucidation of the Reaction Mechanism. Photocatalysts of the type considered in the present work, typified by the oligo-*para*-phenylenes,[14] are promoted to an oxidizing excited state by the incident light. The excited state accepts an electron from the amine and then donates it to the CO_2, with the latter step returning the catalyst to its neutral ground state. The present calculations sought to elucidate what happens next, with a long-term goal of contributing to the design of new photocatalytic systems that might lead to more efficient reduction than those presently explored. Common nonaqueous solvents for this chemistry include dimethylformamide and acetonitrile. In these calculations, the PCM model[23] for acetonitrile was used.

The MP2/aug-cc-pVDZ//MPWB1K/aug-cc-pVDZ model places the dissociated $Et_3N^{\bullet+}$ and $CO_2^{\bullet-}$ radical ions at 82.9−93.4 kcal/mol in enthalpy above the neutral reactants. The range of estimates arises from uncertainty about the correct value to assign to the α parameter, which is a scaling factor for the solvent cavity in the PCM model. The smaller energy difference comes from using the default value of α = 1.2, and the larger uses the value α = 1.35, which has been recommended for calculations on anions.[25] Because the principal challenge in calculations on solvated anions is to avoid solute electron density occupying a volume larger than the solute cavity, an alternative approach (suggested by a reviewer) is to constrain the electrons by avoiding the use of diffuse functions. Hence, MP2/cc-pVDZ//MPWB1K/cc-pVDZ calculations with α = 1.2 were also explored. These placed the radical ions 97.9 kcal/mol above the neutrals. It is hard to know which model is the most reliable, but in any event, even the smallest value of the enthalpy difference suggests that the photocatalyst would need to have an absorption maximum at <345 nm to be able to drive the electron transfer. This is clearly far from optimum if one is considering solar radiation as the energy source, because the maximum in the sea level solar irradiance occurs in the visible region of the spectrum.[26] Longer wavelength light could be used if the amine had a lower oxidation potential, or if some cocatalyst were present that could bind to and stabilize the CO_2 radical anion. The latter seems to occur in systems involving Co or Fe complexes as cocatalysts.[7]

An estimate of ion-pairing energies was obtained by optimizing the structure of triplet $Et_3N^{\bullet+}$ $CO_2^{\bullet-}$. The triplet state was chosen to suppress the back electron transfer. Undoubtedly, many local minima of similar energy exist for this radical ion pair. No effort was made to explore the range of structures, because this was considered to be an issue of marginal importance to the overall study. The particular local minimum that was located in the present work is shown in Figure 3. Its enthalpy placed it 73.6 kcal/mol above the reactants (using α = 1.2, because a single solvent cavity encompasses the overall neutral pair), or 9−20 kcal/mol below the dissociated radical ions. It was assumed that the more chemically relevant singlet radical-ion pair would be similar in enthalpy to the triplet, but the singlet could not be calculated within the present theoretical model.

The next step to be considered was the crucial hydrogen transfer from the amine radical cation to the CO_2 radical anion.

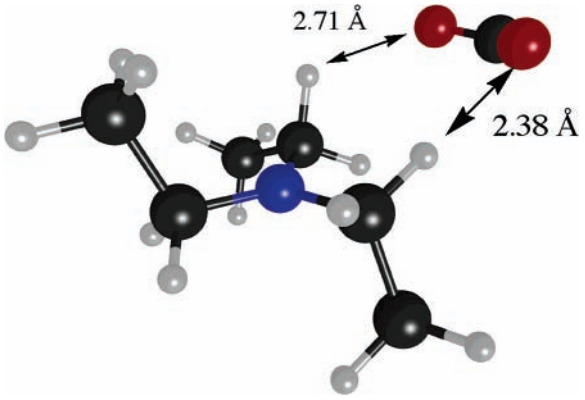

Figure 3. MPWB1K/aug-cc-pVDZ optimized local minimum for the triplet $Et_3N^{\bullet+}$ $CO_2^{\bullet-}$ radical ion pair in acetonitrile.

First, the enthalpy changes for the analogous steps to those listed in Table 1 for the CH_3NH_2 + CO_2 were computed. Not surprisingly, the results for the solution-phase reactions were rather different from the gas-phase ones. The enthalpy difference between HCO_2 and HOCO radicals in acetonitrile was found to be larger than in the gas phase because of the larger dipole moment that HOCO possesses. Thus the $\Delta H°$ values calculated for formation of HCO_2 and HOCO radicals, respectively, were 110.3 and 84.6 kcal/mol with respect to the Et_3N and CO_2 reactants. The double hydrogen transfer, leading to the amino-carbene, was found to be more favorable in acetonitrile ($\Delta H°$ = 48.9 kcal/mol with respect to reactants), because of the large dipole moment for the formic acid product. Of course, the hydride transfer leading to the generation of formate ion was the transformation experiencing the largest solvent effect. In the gas phase it had been by far the most endothermic reaction, whereas it was calculated to be the least endothermic in acetonitrile solution. $Et_2N^+{=}CHCH_3$ and HCO_2^- (α = 1.35) as dissociated ions were calculated to have an enthalpy 36.2 kcal/mol above that of neutral Et_3N and CO_2. As an ion pair, they were found to be only 13.3 kcal/mol above the reactants.

Of the four hydrogen-transfer reactions, two (those forming HCO_2 and HOCO) were calculated to be endothermic with respect to their radical-ion pair precursor, and so presumably would play little role. Of the two exothermic reactions, the one leading to the carbene appeared to be kinetically disfavored. No transition state for a concerted transfer of two hydrogens could be found. Instead, the minimum-energy pathway appeared to be *via* the $Et_2N^+{=}CHCH_3$ and HCO_2^- ion pair. However, as described below, this ion pair has available a more favorable reaction than the one leading to the carbene.

A transition structure for the formation of $Et_2N^+{=}CHCH_3$ and HCO_2^- was located and is depicted in Figure 4. It was found to be higher in enthalpy than the neutral reactants by 26.7 kcal/mol. In other words, it was 46.9 kcal/mol *below* the radical-ion pair and so could not possibly be a transition state directly connecting the $Et_3N^{\bullet+}$ and $CO_2^{\bullet-}$ radical ions with $Et_2N^+{=}CHCH_3$ and HCO_2^- products. That conclusion was reinforced by running an intrinsic reaction coordinate (IRC) calculation from the transition structure. It showed the true reactants to be neutral Et_3N and CO_2. The discovery of the closed-shell transition state for formation of $Et_2N^+{=}CHCH_3$ and HCO_2^- from Et_3N and CO_2 raised the question of how the radical ions could give these same products, and how that reaction, whatever it may be, could compete with simple back electron transfer. Those issues are addressed next.

For any hydrogen transfer between $Et_3N^{\bullet+}$ and $CO_2^{\bullet-}$ to be able to compete with simple return of the radical ion pair to

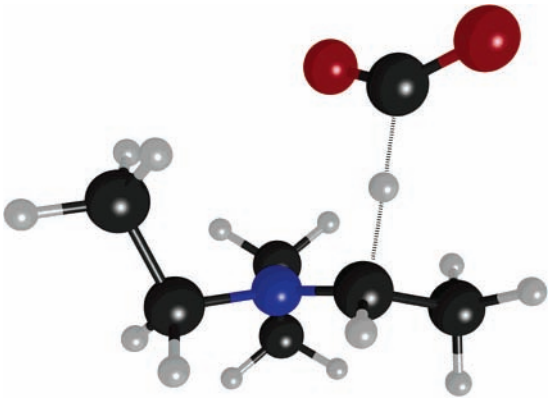

Figure 4. MPWB1K/aug-cc-pVDZ optimized transition structure for formation of $Et_2N^+{=}CHCH_3$ and HCO_2^- in acetonitrile.

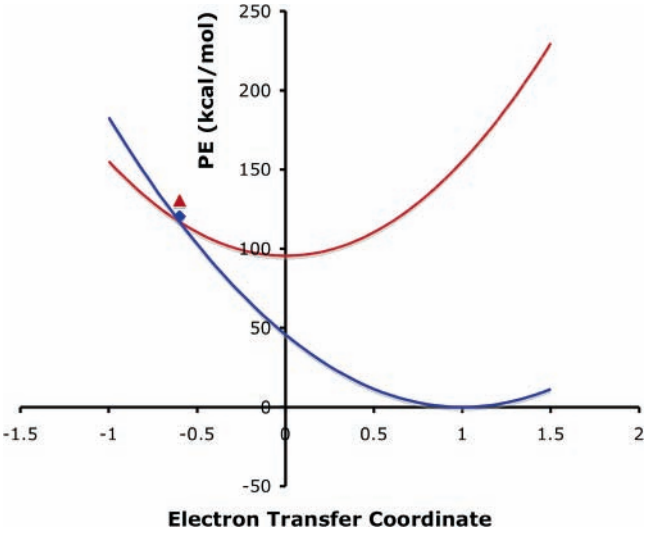

Figure 5. Marcus-type PE parabolas for the outer-sphere back electron transfer between $Et_3N^{\bullet+}$ and $CO_2^{\bullet-}$ in acetonitrile. The upper, red parabola corresponds to the radical ions, and the lower, blue parabola, to the neutral amine and CO_2. See text for further discussion.

the neutral reactants, the outer-sphere back electron transfer presumably must face some sort of barrier. That would be the case if the radical ion pair were in the so-called Marcus inverted region of the rate-constant vs driving-force plot.[27] The key feature of electron-transfer systems in this regime is that at the minimum-energy geometry of the reactant state is electronically excited; i.e., a vertical transition to the product state corresponds to a negative change in standard free energy.

This issue could not be directly probed with free energies in the present calculations, because several of the geometries involved would be far from stationary points on their respective potential energy surfaces. However, a similar question could be posed by calculating potential energies. The results are summarized in Figure 5.

The parabolas in Figure 5 were calculated in the following manner. First, the neutral triethylamine and neutral CO_2 at infinite separation in acetonitrile were assigned a relative energy of [0] and a relative position of [1] on the electron-transfer coordinate. With those two assignments, one parameter remained to calculate the product-state parabola. It was obtained by summing the potential energies of neutral CO_2 at the equilibrium geometry of its radical anion and neutral triethylamine at the equilibrium geometry of its radical cation. For the reactant-state parabola, the $Et_3N^{\bullet+}$ and $CO_2^{\bullet-}$ at infinite separation in acetonitrile were assigned a relative position of [0] on the electron-transfer coordinate, and a relative potential energy equal to their summed PEs minus those for the neutral amine and CO_2 at their respective equilibrium geometries. Again, a third parameter was needed to define the upper parabola, and it was obtained by calculating the PEs of $CO_2^{\bullet-}$ and $Et_3N^{\bullet+}$ at the equilibrium geometries of their respective neutrals. The two parabolas calculated in this manner revealed the classic Marcus "inverted region" intersection at a negative value (−0.598) of the electron-transfer coordinate. This simple picture suggested a barrier of ∼20 kcal/mol to the back electron transfer. The accuracy of the identification of the intersection region by this simple model was assessed in the following manner. The geometries of the neutral pair and of the radical ions, in internal coordinates, were used to define two vectors, **R** and **P**, respectively. A vector, **C**, defining amine and CO_2 geometries at the crossing region was then calculated by

$$\mathbf{C} = \mathbf{R} - 0.598^*(\mathbf{P}-\mathbf{R}) \qquad (1)$$

If the parabola model had been exactly accurate, the energies of the neutrals and of the radical ions should have been identical and should have coincided with the curve crossing on the potential energy axis. The actual results are shown by the triangle (corresponding to the radical ions) and the diamond (corresponding to the neutrals) in Figure 5. Although the coincidence of these points with each other and with the curve crossing is not perfect, it is surprisingly good.

Nevertheless, there are several reasons to be skeptical about the quantitative predictions of the parabola model. First, the electron-transfer coordinate in Marcus theory is generally considered to have an important contribution from solvent reorganization.[28] In the present calculations, that factor is missing, because the PCM calculations yield equilibrium solvation corrections at every point. If nonequilibrium solvation effects could be included, one would expect the result to be increased curvatures of both parabolas, and so to that extent, the neglect of this factor probably results in errors that partially cancel. Second, the reduction of two multidimensional PE hypersurfaces to two parabolas is obviously the grossest of approximations. Rather than there being a single point at which the true surfaces intersect, there will undoubtedly be several seams of intersection, which simply cannot be described in the parabola model. In all probability, the lowest energy intersection between the reactant and product surfaces occurs at a geometry quite unlike the one predicted from the crossing of the parabolas. Finally, the use of potential energies instead of standard free energies in creation of the parabola model means that important entropic effects may have been neglected. Given these serious reservations, it would seem prudent to treat the predicted ∼20 kcal/mol barrier to outer-sphere back electron transfer with appropriate skepticism. However, the qualitative conclusion that the radical ions are in the Marcus inverted region, and consequently face some substantial barrier to outer-sphere electron transfer is probably more reliable.

Even more challenging than trying to identify the mechanism and rate of back electron transfer is the problem of finding the mechanism of hydrogen transfer from the radical ion state. Exploring this issue is a task that should properly involve the use of multiconfigurational electronic-structure methods, such as CASSCF, or better. However, the present problem does not lend itself readily to such techniques, for two reasons. First, the low symmetry of the structures involved and the significant number of lone pairs that could play a role means that a large active space would be needed to be confident of capturing all of the important configurations. Second, as described above, the solvent effect on the ion-pair energies is massive. No

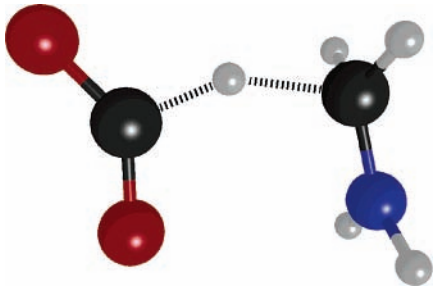

Figure 6. MPWB1K/aug-cc-pVDZ optimized transition structure for the transfer of a hydride ion from methylamine to CO_2 in acetonitrile.

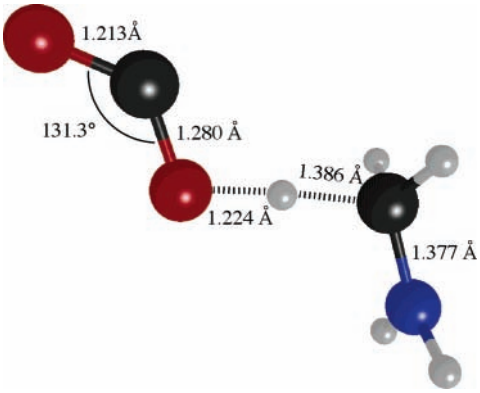

Figure 7. UB3LYP/aug-cc-pVDZ optimized transition structure for C → O hydrogen transfer between methylamine and CO_2 in acetonitrile.

meaningful result could be obtained by searching for conical intersections in the gas phase. However, there are currently few methods available for applying solvent corrections during a conical intersection search. Given these difficulties, a more approximate approach was adopted, again with a view to acquiring qualitative rather than quantitative insight.

Because of the computational overhead involved in searching for the reactive intersection region, the calculations were carried out on the simpler methylamine + CO_2 reaction. The starting point was the C_s symmetry transition structure for hydride transfer from the CH_3NH_2 methyl to the carbon of CO_2, which had already been located during the acquisition of the data for Figure 2. It is depicted in Figure 6. The wave function for this structure seemed to be well described by a single determinant, because an RHF reference for the MP2 calculation was found to be stable with respect to UHF symmetry breaking. Time-dependent DFT, with equilibrium solvation of the excited state,[29] suggested that the energy gap between open- and closed-shell PE surfaces was at least 100 kcal/mol at this geometry. This may seem like an implausibly large value until one recalls that the radicals $HCO_2^{\bullet}$ + $H_2NCH_2^{\bullet}$ are calculated to be almost 100 kcal/mol higher in enthalpy than the ions HCO_2^- + $H_2N^+{=}CH_2$ in acetonitrile.

The very large gap between electronic states at the hydrogen-migration transition structure, and the fact that this gap was substantially larger than that (57.6 kcal/mol) at the geometries of the dissociated radical ions $CH_3NH_2^{\bullet+}$ + $CO_2^{\bullet-}$ made it seem highly unlikely that there could be a crossing of the surfaces anywhere along the reaction coordinate for direct hydrogen transfer between carbons.

The situation was quite different when the hydrogen transfer to oxygen was explored. The transition structure for this reaction (Figure 7) was located with the broken-symmetry UMP2/aug-cc-pVDZ//UB3LYP/aug-cc-pVDZ model. UMPWB1K, which would have been the more consistent choice for the geometry

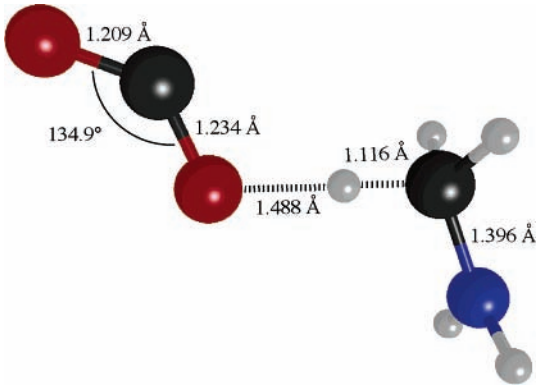

Figure 8. UB3LYP/aug-cc-pVDZ optimized geometry near the crossing of open- and closed-shell PE surfaces for methylamine and CO_2 in acetonitrile.

optimization, was found to be subject to irresolvable convergence failures.

For singlet biradicals, broken-symmetry unrestricted wave functions invariably have high spin contamination, and doubts have been expressed about their validity,[30] although several instances of apparently reliable results from such calculations are now known.[31] In the present case, the $\langle S^2 \rangle$ value at the transition structure was found to be 1.026 for the UMP2 wave function, indicating that this geometry had an open-shell, biradical ground state. However, as described above, the closed-shell neutral state was found to be the lowest in energy at the geometries of the dissociated radical ions, with the PE gap being 57.6 kcal/mol. It follows, therefore, that somewhere along the IRC for the proton transfer summarized by eq 2, there must be

$$H_2N^{\bullet+}CH_2{-}H + CO_2^{\bullet-} \rightarrow H_2NCH_2^{\bullet} + H{-}O{-}C^{\bullet}{=}O \quad (2)$$

a surface crossing. That conclusion was supported by calculating UMP2/aug-cc-pVDZ energies at each point along the UB3LYP/aug-cc-pVDZ IRC for return from the transition structure to the reactants. The $\langle S^2 \rangle$ value of the UMP2 wave function dropped with each step along the path, until it reached zero; i.e., the closed-shell RMP2 solution was found to be the ground state. It is worth noting that the $\langle S^2 \rangle$ value for the wave function from the UB3LYP calculation crossed to zero at the same point in the IRC. The geometry near the crossing point is illustrated in Figure 8.

The question remaining to be addressed was whether the downhill pathways from this crossing point on the closed-shell surface led only to the neutral methylamine and CO_2 reactants (in which case, it would represent merely a path for inner-sphere back electron transfer), or whether there could be a reactive route to $H_2N^+{=}CH_2$ and HCO_2^- from here. Lacking a method for tracking a minimum-energy reaction path from the crossing region, the latter question was addressed in an approximate fashion by calculating a linear-synchronous transit (LST) in internal coordinates between the structures in Figures 8 and 6. The result is shown in Figure 9.

One sees that, although the potential energy does not decrease monotonically along the LST, every point is lower in energy than the first. In view of the small magnitude (1.1 kcal/mol) of the local barrier along the LST, it seems quite probable that there should exist an alternative path in which the energy *would* decrease monotonically between the beginning and end.

These model calculations can be simultaneously summarized and translated to the Et_3N + CO_2 case, as follows. The $CO_2^{\bullet-}$ radical anion approaches the $Et_3N^{\bullet+}$ radical cation preferentially along a path in which the partially negatively charged oxygens

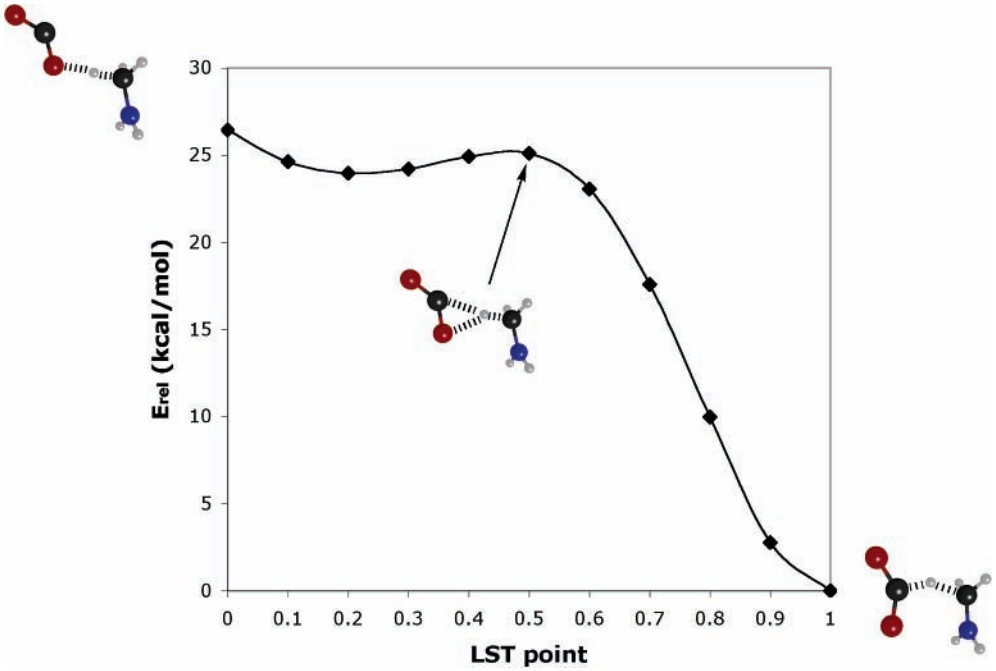

Figure 9. Plot of UMP2/aug-cc-pVDZ energies along a linear-synchronous transit (LST) between the structures in Figure 8 (LST point 0) and Figure 6 (LST point 1).

point toward the amine radical cation. This results in a radical ion pair with a geometry such as that in Figure 3. If the radical-ion pair begins to explore hydrogen transfer from an α carbon of the amine radical cation to an oxygen of the $CO_2^{\bullet-}$ radical anion, it encounters a crossing to the closed-shell PE surface. From this crossing there are downhill paths leading to back electron transfer (giving neutral Et_3N and CO_2) or to hydrogen transfer to the *carbon* of CO_2 (giving $Et_2N^+{=}CHCH_3$ and HCO_2^-). Completion of the hydrogen transfer to oxygen would be uphill on both the open- and closed-shell surfaces and so is disfavored.

The branching ratio between back electron transfer and hydrogen transfer is obviously an important issue in determining the overall efficiency of the photochemical CO_2 reduction. Unfortunately, the present calculations are unable to provide insight into that issue, although some issues that may influence the ratio are discussed below. Quantitative prediction of the branching ratio would presumably require a nonadiabatic molecular dynamics simulation. From the $Et_2N^+{=}CHCH_3/HCO_2^-$ ion pair, the favored hydrogen transfer gives $Et_2NCH{=}CH_2$ + HCO_2H, rather than the carbene Et_2NCCH_3 + HCO_2H, although both reactions are calculated to be endothermic with respect to the ion pair. However, because Et_3N is a stronger base than $Et_2NCH{=}CH_3$, the reaction could be driven toward the diethylvinylamine by deprotonation of the formic acid with unreacted triethylamine. A summary of the computed enthalpy changes is shown in Figure 10.

Prediction of an Improved Reaction with a Modified Amine. One problem that the present calculations have highlighted in the use of triethylamine as reductant in the solar conversion of CO_2 to formate is the high energy of the dissociated $Et_3N^{\bullet+}$ and $CO_2^{\bullet-}$ radical ions, the magnitude of which leads to the conclusion that only light of wavelength <345 nm could drive the reaction. Another is that the crossing from the open-shell to the closed-shell surface, which is believed to be responsible for the desired reaction, also permits unproductive inner-sphere back electron transfer. It is then interesting to ask whether there are modifications to the reaction that could improve the reduction efficiency. One widely explored approach is to introduce transition-metal photocatalysts or cocatalysts, which are capable of binding CO_2 and making it more easily reduced.[32−36] An alternative, which appears to have been much less thoroughly investigated, would be to examine changes to the structure of the amine. Because, in the end, the ideal system would be one allowing the regeneration of the amine in a separate photochemical step, even relatively expensive or difficult-to-synthesize amines could potentially be economically viable.

Obviously, the number of possible changes to the structure of the amine that could be made is vast. For the purposes of the present study, only a single modification was explored. It was the incorporation of the amine into a bicyclic skeleton. The motivation for this choice was the report by Aue and co-workers that the ionization potential for 1-azabicyclo[3.3.3]undecane (ABU, or manxine) was much lower than that for acyclic tertiary amines.[37] Subsequently, the oxidation potential of ABU in aqueous methanol was found to be 0.35 V lower than that of triethylamine.[38] The generally accepted explanation for these observations is that the bridgehead nitrogen of ABU is forced to adopt a near-planar local geometry, and that this raises the energy of the lone pair and so reduces the ionization and oxidation potentials.[37] MPWB1K/aug-cc-pVDZ geometry optimizations (again in a PCM representation of acetonitrile) certainly supports that analysis: for triethylamine, the nitrogen was found to be 0.418 Å out of the plane of its three α carbons, whereas for ABU the corresponding value was only 0.176 Å. MP2/aug-cc-pVDZ//MPWB1K/aug-cc-pVDZ enthalpy calculations suggested that the $ABU^{\bullet+}$ and $CO_2^{\bullet-}$ dissociated radical ions should be 73.4−83.9 kcal/mol (again, depending on the value of α used for the radical anion) above the neutrals in acetonitrile, with the lower value implying a threshold of about 390 nm for the absorption maximum of any photocatalyst for the electron transfer. This is on the edge of the visible spectrum.

It is perhaps worth noting that the $^3(n,\pi^*)$ state of benzophenone is more efficiently reduced by ABU than by triethylamine.[39] This reaction initially follows an electron-transfer mechanism, like that proposed for CO_2 reduction, but the radical ion pair then undergoes proton rather than hydrogen-atom

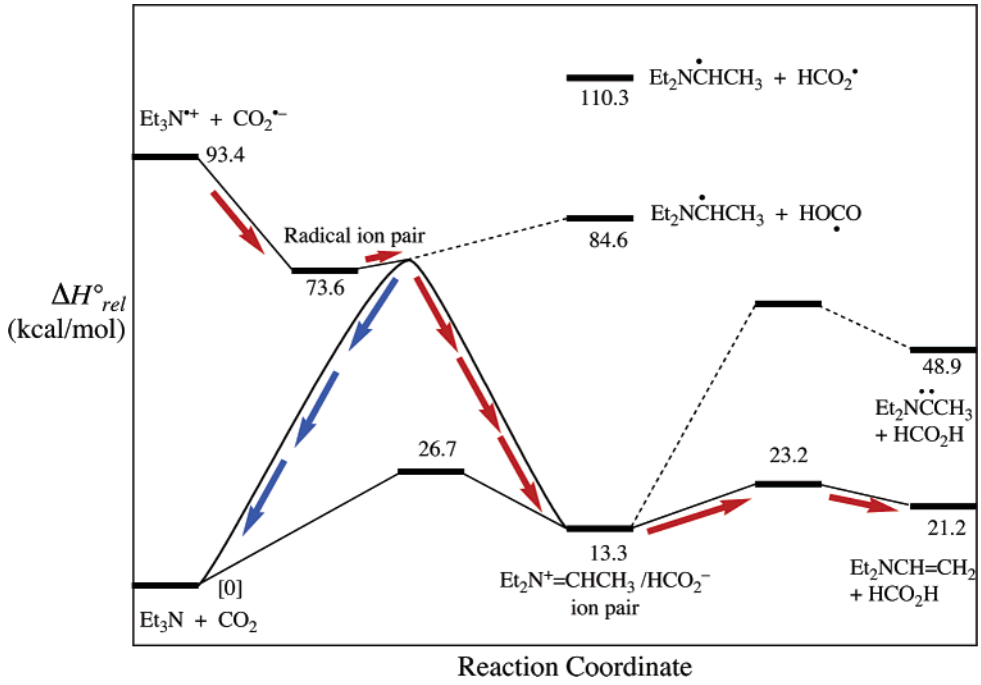

Figure 10. MP2/aug-cc-pVDZ//MPWB1K/aug-cc-pVDZ enthalpy profiles for reduction of CO_2 with triethylamine in acetonitrile. The red arrows show the predicted reactive path, and the blue arrows show inner-sphere back electron transfer.

transfer, and so an analogy between the two reductions should be drawn only with caution.

Clearly there are many more structural and constitutional variations that could be considered for the amine. It seems very likely that with an optimized choice, high efficiency reduction of CO_2 using visible light should be possible. Calculations of the type reported here could be helpful in guiding that optimization, although the crucial issue of the ratio of hydrogen transfer to back electron transfer at the surface crossing is not something that is easily predicted at this stage. Almost certainly, a combined experimental and computational study would be the most reliable way to tune the amine properties.

Conclusions

The principal conclusions drawn from the present calculations are as follows.

1. The radical ions $Et_3N^{\bullet+}$ and $CO_2^{\bullet-}$, generated with the aid of a photocatalyst in a polar solvent such as acetonitrile, are probably in the Marcus inverted region of the rate constant vs driving force plot and, hence, should face a barrier to outer-sphere back electron transfer,

2. There appears to be no crossing of excited-state and ground-state potential energy surfaces along a coordinate for reduction of CO_2 in which the hydrogen transfer occurs directly between carbons.

3. Along a coordinate for transfer of a hydrogen from an α carbon of $Et_3N^{\bullet+}$ to an *oxygen* of $CO_2^{\bullet-}$ there probably is a crossing of excited-state and ground-state potential energy surfaces. From this intersection region there appear to be downhill paths for inner-sphere back electron transfer and for reduction, but with the latter involving attachment of the hydrogen to the *carbon* of CO_2.

4. In the gas phase, the least endothermic reaction for reduction of CO_2 by a tertiary amine involves transfer of *two* α hydrogens, generating formic acid and an aminocarbene. However, in polar solvents the overall hydride transfer (with respect to neutral reactants) giving formate ion and an iminium ion is the least endothermic reaction.

5. Structural modifications of the amine could lead to more efficient reduction with longer wavelength light. One step in that direction seems to be inclusion of the amine in a bicyclic skeleton, such as that offered by 1-azabicyclo[3.3.3]undecane.

Acknowledgment. This is the author's last paper resulting from research conducted under a grant from the U.S. Department of Energy (present grant DE-FG02-98ER14857). The author expresses his great appreciation for the intellectual and material support that the members of the DOE Combustion Research program have provided for his work over the years.

Supporting Information Available: Cartesian coordinates and energies of stationary points for reactions discussed in this paper, plus a full citation for ref 24. This material is available free of charge via the Internet at http://pubs.acs.org.

References and Notes

(1) Mitchell, J. F. B.; Lowe, J.; Wood, R. A.; Vellinga, M. *Philos. Trans. R. Soc. A* **2006**, *364*, 2117−2133.

(2) Goldemberg, J. *Energ. Policy* **2006**, *34*, 2185−2190.

(3) Bearat, H.; McKelvy, M. J.; Chizmeshya, A. V. G.; Gormley, D.; Nunez, R.; Carpenter, R. W.; Squires, K.; Wolf, G. H. *Environ. Sci. Technol.* **2006**, *40*, 4802−4808.

(4) Wu, J. C. S.; Lin, H. M.; Lai, C. L. *Appl. Catal. A* **2005**, *296*, 194−200.

(5) Shen, Y. M.; Duan, W. L.; Shi, M. *J. Org. Chem.* **2002**, *68*, 1559−1562.

(6) Grodkowski, J.; Neta, P.; Fujita, E.; Mahammed, A.; Simkhovich, L.; Gross, Z. *J. Phys. Chem. A* **2002**, *106*, 4772−4778.

(7) Dhanasekaran, T.; Grodkowski, J.; Neta, P.; Hambright, P.; Fujita, E. *J. Phys. Chem. A* **1999**, *103*, 7742−7748.

(8) Behar, D.; Dhanasekaran, T.; Neta, P.; Hosten, C. M.; Ejeh, D.; Hambright, P.; Fujita, E. *J. Phys. Chem. A* **1998**, *102*, 2870−2877.

(9) Koike, K.; Hori, H.; Ishizuka, M.; Westwell, J. R.; Takeuchi, K.; Ibusuki, T.; Enjouji, K.; Konno, H.; Sakamoto, K.; Ishitani, O. *Organometallics* **1997**, *16*, 5724−5729.

(10) Fujita, E.; Brunschwig, B. S.; Ogata, T.; Yanagida, S. *Coord. Chem. Rev.* **1994**, *132*, 195−200.

(11) Hirota, K.; Tryk, D. A.; Hashimoto, K.; Okawa, M.; Fujishima, A. *J. Electrochem. Soc.* **1998**, *145*, L82−L84.

(12) Kohno, Y.; Yamamoto, T.; Tanaka, T.; Funabiki, T. *J. Mol. Catal. A* **2001**, *175*, 173−178.
(13) Tachikawa, T.; Tojo, S.; Fujitsuka, M.; Majima, T. *Langmuir* **2004**, *20*, 9441−9444.
(14) Matsuoka, S.; Kohzuki, T.; Pac, C.; Ishida, A.; Takamuku, S.; Kusaba, M.; Nakashima, N.; Yanagida, S. *J. Phys. Chem.* **1992**, *96*, 4437−4442.
(15) Dunning, T. H. *J. Chem. Phys.* **1989**, *90*, 1007−1023.
(16) The present calculations used the Gaussian 03 variant of B3LYP. See: Hertwig, R. H.; Koch, W. *Chem. Phys. Lett.* **1997**, *268*, 345−351.
(17) Zhao, Y.; Truhlar, D. G. *J. Phys. Chem. A* **2004**, *108*, 6908−6918.
(18) Møller, C.; Plesset, M. S. *Phys. Rev.* **1934**, *46*, 618−622.
(19) Montgomery, J. A.; Ochterski, J. W.; Petersson, G. A. *J. Chem. Phys.* **1994**, *101*, 5900−5909.
(20) Scott, A. P.; Radom, L. *J. Phys. Chem.* **1996**, *100*, 16502−16513.
(21) Blanksby, S. J.; Ellison, G. B. *Acc. Chem. Res.* **2003**, *36*, 255−263.
(22) Dixon, D. A.; Arduengo, A. J. *J. Phys. Chem. A* **2006**, *110*, 1968−1974.
(23) Barone, V.; Cossi, M. *J. Phys. Chem. A* **1998**, *102*, 1995−2001.
(24) Frisch, M. J.; et al. *Gaussian 03*, revision D.02; Gaussian, Inc.: Wallingford, CT, 2004.
(25) Pliego, J. R.; Riveros, J. M. *Chem. Phys. Lett.* **2002**, *355*, 543−546.
(26) Pap, J. M.; Frohlich, C. *J. Atmos. Sol.-Terr. Phys.* **1999**, *61*, 15−24.
(27) Siders, P.; Marcus, R. A. *J. Am. Chem. Soc.* **1981**, *103*, 748−752.
(28) Marcus, R. A. *J. Phys. Chem. B* **1998**, *102*, 10071−10077. See also the article by Nelsen and Blomgren that discusses solvent and other contributions to the reorganization energy. It uses an approach to estimate their magnitude that is akin to the one used here. Nelsen, S. F.; Blomgren, F. *J. Org. Chem.* **2001**, *66*, 6551−9.
(29) Scalmani, G.; Frisch, M. J.; Mennucci, B.; Tomasi, J.; Cammi, R.; Barone, V. *J. Chem. Phys.* **2006**, *124*, 094107/1−15.
(30) Kozlowski, P. M.; Dupuis, M.; Davidson, E. R. *J. Am. Chem. Soc.* **1995**, *117*, 774−778.
(31) See, for example: Ozkan, I.; Kinal, A.; Balci, M. *J. Phys. Chem. A* **2004**, *108*, 507−514. Successful uses of broken-symmetry UHF references for MP2 calculations can be found in: Crawford, D. T.; Kraka, E.; Stanton, J. F.; Cremer, D. *J. Chem. Phys.* **2001**, *114*, 10638−50. Isobe, H.; Takano, Y.; Kitagawa, Y.; Kawakami, T.; Yamanaka, S.; Yamaguchi, K.; Houk, K. N. *J. Phys. Chem. A* **2003**, *107*, 682−94.
(32) Lehn, J. M.; Ziessel, R. *Proc. Natl. Acad. Sci. U.S.A.* **1982**, *79*, 701−4.
(33) Ziessel, R. *NATO ASI Ser. C* **1990**, *314*, 79−100.
(34) Matsuoka, S.; Yamamoto, K.; Ogata, T.; Kusaba, M.; Nakashima, N.; Fujita, E.; Yanagida, S. *J. Am. Chem. Soc.* **1993**, *115*, 601−9.
(35) Hori, H.; Ishitani, O.; Koike, K.; Johnson, F. P. A.; Ibusuki, T. *Energ. Conv. Manag. 1995*, *36*, 621−4.
(36) Ogata, T.; Yanagida, S.; Brunschwig, B. S.; Fujita, E. *J. Am. Chem. Soc.* **1995**, *117*, 6708−16.
(37) Aue, D. H.; Webb, H. M.; Bowers, M. T. *J. Am. Chem. Soc.* **1975**, *97*, 4136−4137.
(38) Lindsay Smith, J. R.; Masheder, D. *J. Chem. Soc., Perkin Trans. 2* **1976**, 47−51.
(39) Von Raumer, M.; Suppan, P.; Haselbach, E. *Helv. Chim. Acta* **1997**, *80*, 719−724.